sciendo

DOI: 10.2478/auoc-2025-0001

Ovidius University Annals of Chemistry Volume 36, Number 1, pp. 1 - 12, 2025

Adsorption and desorption performances of *Eichhornia crassipes* (water hyacinth) roots and leaves powder towards metal ions in industrial wastewater

Godswill O. TESI*,[1] Onome EJEROMEDOGHENE,[2] Yakubu A. ALLI,[3,4] Happiness B. OKUNOJA,[5] and Ayodele R. IPEAIYEDA[6]

[1]*Department of Chemistry, Federal University of Petroleum Resources, Effurun, Delta State, Nigeria*
[2]*College of Chemistry, Chemical Engineering and Materials Science, Soochow University, Suzhou 215123, China*
[3]*Laboratoire de Chimie de Coordination du CNRS, UPR8241, Universite´ de Toulouse, UPS, INPT, Toulouse cedex 4 F-31077, France*
[4]*Department of Chemical Sciences, Faculty of Science and Computing, Ahman Pategi University, Km 3, Patigi-Kpada Road, Patigi, Kwara State 243105, Nigeria*
[5]*Department of Chemistry, Delta State University, Abraka, Nigeria*
[6]*Department of Chemistry, University of Ibadan, Ibadan, Nigeria*

Abstract. This study investigated the adsorption and desorption performances of water hyacinth leaves powder (WHLP) and water hyacinth roots powder (WHRP) towards Pb^{2+}, Co^{2+}, Zn^{2+} and Ni^{2+} in industrial wastewater. The parameters influencing the process were assessed, models were proposed to explain the both the equilibrium and kinetics of the sorption process and desorption study was conducted using different HNO_3 and NaOH concentration. The results showed that comparatively, the metal uptake capacity of water WHLP was higher than WHRP as examined by the investigated parameters. The biosorption data fitted to both Langmuir and Freundlich isotherms. The kinetics of the process follows a pseudo-second order reaction model because it provides good linearization of the experimental data. In addition, relatively successful metal ions desorption from the biosorbents were recorded with both NaOH and HNO_3 solutions.

***Keywords*:** water hyacinth; adsorption; industrial wastewater; desorption.

1. Introduction

Metals are a class of environmental contaminants and many of them are very harmful even at low levels. However, there has been increased pollution of the biosphere with dangerous metals due to man's enormous and sustained industrial activities [1, 2]. Typically, environmental pollution arises from the smelting of metals, consumption of fossil fuels, pesticides, municipal wastes, fertilizers, and sewage [3]. Metals are a major source of concern, owing to their recognized toxicity to aquatic life and human health at very low concentrations [4–6]. According to Zhou *et al.* [7] and Akhtar *et al.* [8], industrial discharges are likely the most prominent anthropogenic source of metals in the aquatic environment. However, a fundamental shortcoming in estimating metals' fate and transit in wastewater treatment processes is the lack of a reliable way to predict metals distribution in treatment units, necessitating the establishment of effective pre-treatment guidelines [9].

Industrial growth and other human activities in some emerging nations, along with an immense and expanding demand for metals like cadmium, lead, chromium, zinc, copper, and nickel results in significant levels of pollution in water bodies [10, 11]. Metals in wastewater, unlike organic pollutants, are not easily destroyed by biological processes, and they display effects on both humans and aquatic ecosystems via the pollution of drinking water [12]. The reuse of cleansed wastewater is a vital approach to saving water-based resources, situated in areas prone to water scarcity.

In the quest to mitigate the unpleasant consequences of metals present in water bodies, numerous research has found that man-made wetlands are quite efficient in removing metals from wastewater emanating from industrial sources [13–15]. However, marked differences have been seen in the ability of diverse plant species found in the wetland to absorb and retain certain metals of interest [16]. For example, wetland plant species such as water hyacinths with strong trace element removal capacities from water have been reported [17].

Water hyacinth (*E. crassipes*), a member of the Pontederiaceae family, grows abundantly in certain regions of the world such as Africa, the Pacific, Southeast Asia, the Caribbean, and Latin America [18, 19]. When employed as a biological filtration system, water hyacinth, like most macrophytes that grow in aquatic environments, has displayed a high capacity for removing contaminants as it possesses numerous sites for binding metallic ions and complexes [20, 21]. These sites include sulfate, imidazole, hydroxyl, amine, phosphate, sulfhydryl, carboxyl, and other chemical functional groups present in their cellular sugar and

*Corresponding author. *E-mail address:* godswillinfodesk@yahoo.com (Godswill O. Tesi)

protein [22, 23]. Water hyacinth has shown great potential in the absorption and bio-concentration of a wide range of hazardous metals from aquatic settings. As a result, throughout the last few decades, there has been an increase in plant usage studies [24].

The biosorption course usually comprises two phases: a solid phase (biosorbent) and water (or other solvents) as a liquid phase in which components to be adsorbed are dissolved [25, 26]. Metal-sequestering properties of biosorbent materials can be exploited to reduce metal ion concentrations in solution [27, 28]. The advantages of this process over other methods include high efficiency and high likelihood of recovering the metals after adsorption, reduced cost, absence of nutrition requirement, reduced biological/chemical sludge, and biosorbent regeneration [29]. Previous research has shown that the dried biomass of water hyacinth may effectively remove metals from contaminated solutions [30-33]. Hemalatha *et al.* [32] found that the biosorbent prepared from root of water hyacinth showed maximum Zn removal of 98.9% and stem showed Cr removal of 96.4%. As a result, the overarching goal of this research is to see how effective dried roots and leaves of water hyacinth are, at removing metals (Zn^{2+}, Ni^{2+}, Co^{2+}, and Pb^{2+}) from industrial effluent.

2. Experimental

2.1. Materials and reagents

The water hyacinth plant was harvested from Oba Dam, Ibadan. The reagents (nitric acid, sodium hydroxide, hydrochloric acid, EDTA and stock solution of metals) were purchased from Merck, Darmstadt, Germany.

2.2. Water hyacinth leaves and roots adsorbent preparation

The collected water hyacinth leaves and roots used in the study were washed severally with tap water, dried in the open air for several days, and grounded to powder with an electric blender. Thereafter, they were sieved using a 2 mm sieve before being employed for the metal ion sorption without further pretreatment. The prepared adsorbents were denoted as WHLP and WHRP for water hyacinth leaves and roots powders respectively.

2.3. Characterization of biosorbents

The structural characterization of the biosorbents was evaluated with KBr pellets using FT-IR TENSOR27 PMA 50 (manufactured by Brook, Germany). A 4.0 cm^{-1} resolution over 32 scans ranging from 4000-400 cm^{-1} was used. Biosorbent morphology was assessed on an FEI Sirion Scanning Electron Microscope (SEM) and FEI Tecnai G2 20 transmission electron microscope (TEM) that operated at a voltage of 200 kV.

2.4. Preparation of adsorbate

The metal ion adsorbate stock solution was made by dissolving a predetermined amount of the metal salts into a 1 L volumetric flask with distilled water. This was followed by the standardization of the stock solution using standard 0.01M EDTA solution, a suitable indicator, and buffer solution of pH 10. From the stock solution, working solutions containing equal molar quantities of the metal ions (samples) were made ready by diluting the stock solution using distilled water. Each sample was analyzed in triplicate to reduce experimental error and obtain reproducible results; while the metal ion quantities in the different samples were determined using Perkin Elmer-manufactured AAS (Atomic Absorption Spectrophotometer) Analyst 200, USA. The wavelength values for metals determination were 213.9, 232, 240.7 and 283.3 nm for Zn^{2+}, Ni^{2+}, Co^{2+}, and Pb^{2+} respectively. The accuracy of the analytical procedure was evaluated by using a spike recovery method. Already analyzed samples were spiked with a known concentration of metal ions and the samples reanalyzed. The percent spike recoveries for the metal ions were between 96.4% and 102%. Metal ions determination was performed in triplicate and the relative standard deviations (RSD) for the triplicate analyses were < 10%. The R^2 values of the calibration lines for the metals varied between 0.9995 and 0.9999.

2.5. Batch adsorption experiments

The optimization of the conditions was carried out according to already established procedures [33-35]. The effect of pH on the biosorbent was assessed by adding 1.0 g of the powdered biosorbents to 25 mL of the metal ions (sample) solution in a flask. The pH of these suspensions was attuned to 4.0, 5.0, 6.0, 7.0, 8.0, and 9.0 using 2M NaOH or 2M HCl solution. Also, the influence of biosorbent contact time was assessed by measuring 1 g of the powdered biosorbents into different flasks for the different contact time frames of 15, 30, 45, 60, 75, and 90 min. Thereafter, 25 mL of the prepared metal ion solution containing equal concentration (5 mg/L) at pH 7 was added to the container and shaken at 30 ^{o}C. The effect of the biosorbent dosage was determined by mixing various sizes of the powdered biosorbent (0.2, 0.4, 0.6, 0.8, 1.0, and 1.2 g) with 25 mL of the metal ion solution with the pH adjusted to 7 in a separate flask. In addition, several standard solutions containing an equal concentration of the metal ions were prepared; while 1.0 g of the biosorbents was weighed into several flasks to determine the influence of the starting heavy metal concentration on the adsorption performance. Next, 25 mL of the prepared metal ions solutions (with the pH adjusted to 7) containing an equal concentration of 5 mg/L was added to the flasks. In all these processes, the obtained mixtures were shaken for one hour with the aid of a rotary shaker at 30 ^{o}C. Thereafter, it was filtered by gravity with filter paper (Whatman No. 1). The concentration of the metal ions in the filtrate was subsequently determined with AAS as described previously [33-35].

2.6. Desorption studies

The desorption study was carried out with different concentrations (2 M, 4 M, and 6 M) of HNO_3 and NaOH. Briefly, 25 mL of a mixture of the recovered biosorbent and adsorbate was shaken for 1 h and left undisturbed for one day. Thereafter, the solutions were filtered and the metal ions concentrations were evaluated by AAS.

The desorption percentages were computed according to this formula (Eqn. 1):

$$Efficiency\ of\ desorption\ (\%) = \frac{released\ metal\ concentration}{initially\ sorbed\ metal\ concentration} x100 \quad (1)$$

3. Results and discussion

3.1. Description of the biosorbents

The morphology of the WHLP and WHRP obtained were investigated using SEM.

The SEM micrograph of WHLP revealed aggregated layers with wide porous construction (Fig. 1a) [36]. However, the WHRP show aggregated fiber bundles (Fig. 1b). The observed porous construction could serve as sites where sorption of toxic metal ions takes place [37]. More also, the TEM images further reveal the uniform serpentine-like morphology due to the interconnected fibrous structures in the adsorbents (Fig. 1c-d).

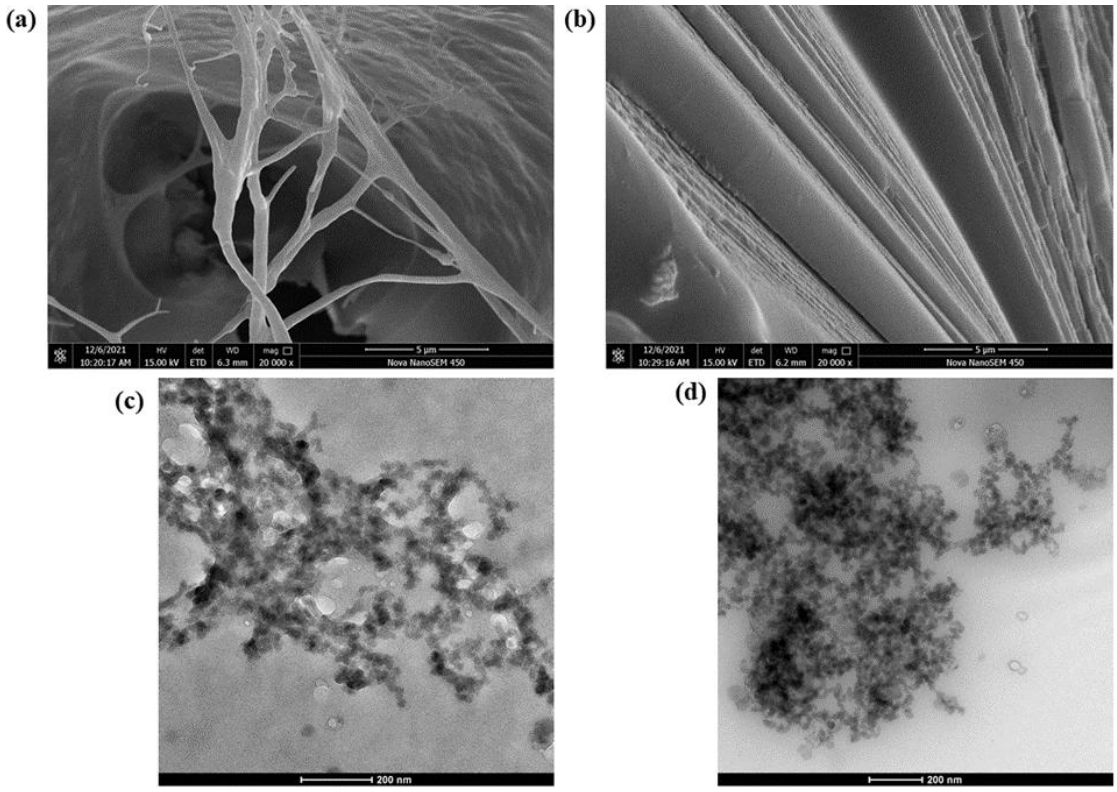

Figure 1. SEM and TEM images of water hyacinth (a/c) root and (b/d) leaves powders respectively

3.2. Effect of pH

Scholars have shown that the pH of a particular medium influences how soluble metal ions can be in the medium. It also influences the number of measurable counter ions present on the functional groups of the sorbent cell walls. For this reason, it can be said that pH is a vital process index involved in the sorption of ions of metals from aqueous solutions considering the fact that it accounts for the protonation of sites where metals can bind, the solubility of calcium carbonate and speciation of metals in the solution [38].

This study revealed that Zn, Co, Pb, and Ni, uptake by WHLP and WHRP increased as pH increased in value from 4 to 7 (Fig. 2a-b). Beyond pH 7 there was not much further increase in the uptake efficiency. Comparable results have also been reported in the works of literature on various sorbent systems [39–41]. This observed boost in the sorption accompanying increase in pH can be attributed to the mechanism displayed in ion-exchange sorption in which a vital role is performed by ligands possessing cation-exchange properties. The removal of the metals (Zn, Co, Pb, and Ni) was hindered at lesser pH ranges. The reason for this may be the antagonism of H^+ and metal ions on the sorption sites, with a clear predominance of H^+, which blocks the approach of positive metal ions as a result of the repulsive force. At higher pH, ligands like carbonate groups in the biosorbent are uncovered, thereby causing an increase in the negative charge density available on the surface of the sorbent with a resultant boost in the pull of metallic ions having a net positive charge and facilitating their sorption onto the surface of the sorbent. As seen in this research, the examined metal cations (as pH approached 7) may have interacted intensely with the binding sites in the WHLP and WHRP that are negatively charged. Going by this, pH 7 was the optimum pH for the metal sorption and as such, the remaining adsorption experiments were executed at pH 7.

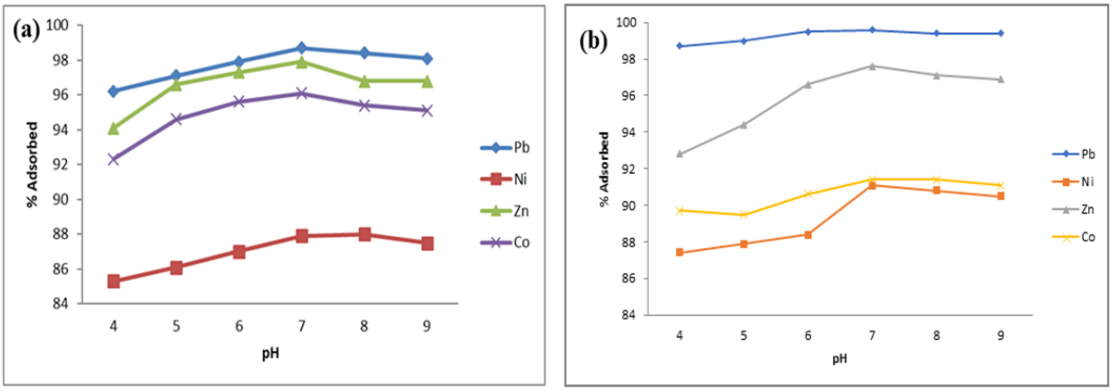

Figure 2. Influence of pH on metal ions sorption by (a) WHLP and (b) WHRP

3.3. Influence of time of contact

Time of contact has a vital function in the resourceful removal of metals using WHLP and WHRP. The influence of contact time on the biosorption capacity for the diverse metals and with the different biosorbents was investigated. The results show that the metal sorption using water WHLP increases for Pb^{2+} from 99.2 % to 99.5 %, Ni^{2+} from 86.0 % to 87.5 %, Zn^{2+} from 91.8 % to 95.3 %, and Co^{2+} from 91.7 % to 93.0 % as the time of contact move from 15 to 90 min (Fig. 3a). Meanwhile, the WHRP displayed an increased removal efficiency for Pb^{2+} from 98.3 % to 98.7 %, Co^{2+} from 81.9 % to 89.0 %, Zn^{2+} from 89.5 % to 91.0 %, and Ni^{2+} from 92.1 % to 95.7 %, as the time of contact move from 15 to 90 min (Fig. 3b).

The result vividly exposed that the adsorption rate is superior at the starting point and this is due to the availability of a huge number of active sites on the adsorbent surface. As these sites are used up, the rate of uptake is controlled by the speed at which the adsorbate is moved to the interior sites of the particles involved in the adsorption from the exterior [29]. Maximum removal was achieved within the initial 60 min of the time of contact and the sorption did not change appreciably with further augmenting in the time of contact. Going by this, the remaining sorption studies were executed at 60 min time of contact. The equilibrium time needed by the adsorbents employed for this study was reduced, compared to some values recorded in the literature [42]. This is noteworthy because equilibrium time is an indispensable factor considered for waste and economical applications. In process application, this fast (or immediate) biosorption phenomenon has great advantages since shorter the time of contact successfully allow for the use of smaller contact equipment, and this in turn greatly influences both the operation competence cost of the process.

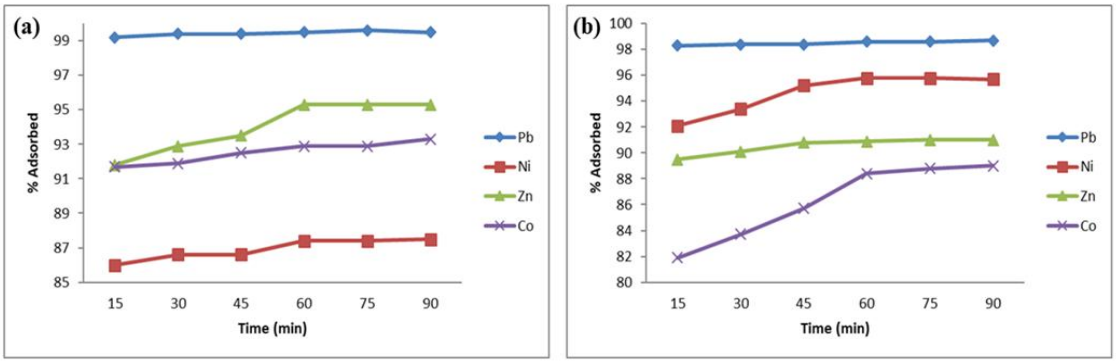

Figure 3. Influence of time of contact on metal ions sorption by (a) WHLP and (b) WHRP

3.4. Effect of initial metal ion concentration

A biosorption process' viability and effectiveness are influenced by the concentration of the metal ion solution in addition to the characteristics of the biosorbents [43]. A significant force is provided by the initial metal ion concentration to overcome all the metal mass transfer resistances between the aqueous and solid phases [44]. The effect of the initial concentration of metal ions shows that the removal efficiency decreased slightly for Pb^{2+} from 99.8 % to 99.3 %, and Zn^{2+} from 95.9 % to 93.4 %, as well as a wide decrease in Ni^{2+} from 86.3 % to 63.2 %, and Co^{2+} from 93.6 % to 84.6 % as the initial metal ions concentration increases from 5 mg/L to 30 mg/L using WHLP as biosorbent (Fig. 4a). For WHRP, the metal ion removal efficiency reduces as regards Pb^{2+} from 99.4 % to 98.7 %, Co^{2+} from 87.1 % to 80.2 %, Zn^{2+} from 97.7 % to 93.2 %, and Ni^{2+} from 85.0 % to 63.0 % as the concentration of starting metal ions rises from 5 mg/L to 30 mg/L (Fig. 4b).

The adsorbate concentration effect can result from a variety of sources. First, during the adsorption reaction, adsorption sites remain unsaturated. Meanwhile, agglomeration of adsorbent particles at increasing concentrations could be another cause. Such aggregation results in an increase in the diffusional path length and a decrease in the overall surface area of the adsorbent particles available for adsorption [45]. The proportion of sorption was higher at lower concentrations of metal ions because all of the metal ions in the solution could interact with the binding sites. Lower adsorption yield at

greater concentrations is caused by saturating adsorption sites. As a result, the dilution of waste fluids with a high concentration of metal ions can boost the yield of purification [46].

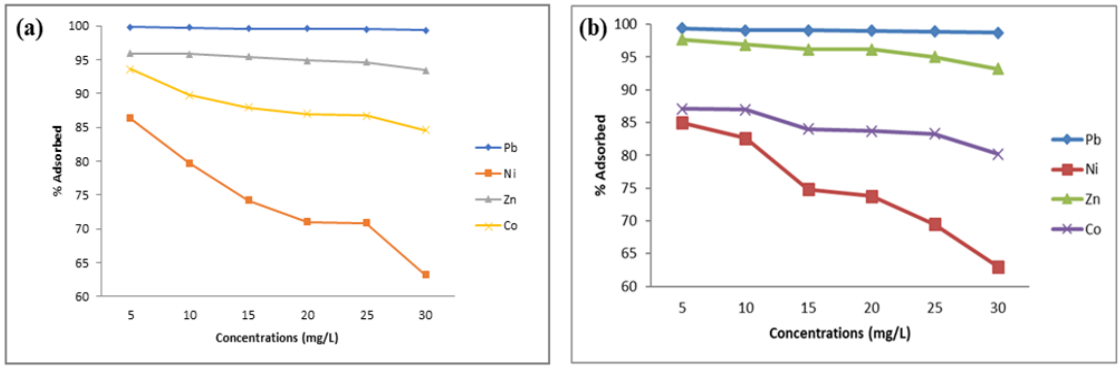

Figure 4. Influence of initial metal ion concentration on the sorption of metal ions by (a) WHLP and (b) WHRP

3.5. Influence of dosage

The influence of varying the biosorbent dosage on the sorption of the different metal ions is depicted in Fig. 5a-b. It was seen that the efficiency of removal increases correspondingly as the mass of the biosorbent increases [47]. The increase in sorbent surface area and ion binding sites causes a clear increase in the amount of solute that was absorbed [42, 48]. For WHLP, the removal competence increases in Ni^{2+} from 87.5 % to 91.7 %, Pb^{2+} from 82.1 % to 98.9 %, Zn^{2+} from 87.2 % to 96.2 %, and Co^{2+} from 93.1 % to 96.2 % as the dosage increases from 0.2 g to 1.2 g at a first metal ion concentration of 5 mg/L, while for WHRP, the efficiency of removal increases for Ni^{2+} from 99.5 % to 99.8 %, Pb^{2+} from 99.3 % to 99.9 %, Zn^{2+} from 99.7 % to 99.8 %, and Co^{2+} from 99.4 % to 99.7 % as the dosage increases from 0.2 g to 1.2 g at an initial metal ion concentration of 5 mg/L.

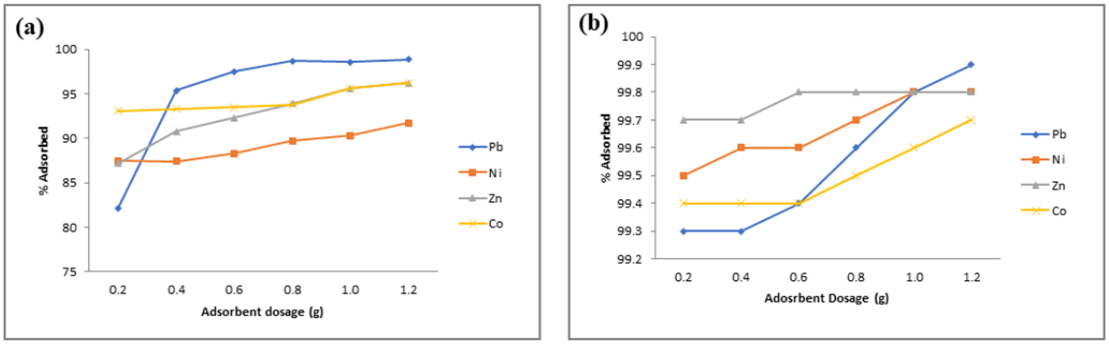

Figure 5. Influence of adsorbent dosage on the sorption of metal ions by (a) WHLP and (b) WHRP

3.6. Adsorption equilibrium

The investigation of the metal-adsorbent sorption system utilized both the Freundlich and Langmuir adsorption isotherm equilibrium models.

3.6.1. Langmuir isotherm

The maximum adsorption capacity of the adsorbent Q_m (mg/g) and a parameter (K_a) related to the affinity of the binding sites (l/mg) were calculated using the rearranged Langmuir's adsorption isotherm model for analyzing the monolayer sorption processes [49] shown in Eqn. 2.

$$\frac{C_e}{q_e} = \frac{1}{Q_m \cdot K_a} + \frac{C_e}{Q_m} \qquad (2)$$

Where: q_e = metal ions concentration on biosorbent (mg/g) at equilibrium; C_e = metal ions concentration in solution (mg/L) at equilibrium; Q_m is the maximum sorption upon complete saturation of the biosorbent surface (mg/g); K_a is a constant related to the adsorption /desorption energy (L/mg).

The plot of C_e/q_e against C_e for Pb^{2+}, Ni^{2+}, Zn^{2+}, and Co^{2+} for all the adsorbents used are shown in Fig. S1a-d and Fig. S2a-d, and the Langmuir isotherm parameters Q_m, K_a, K_R, and the regression coefficient (R^2) are shown in Tables 1-2.

The linear plot of the C_e/q_e against C_e shows that the adsorption of the four metal ions by WHLP and WHRP fits well with the Langmuir model.

The values of the R^2 obtained ranging from 0.893 to 0.981 for WHLP (Table 1) and 0.925 to 0.987 for WHRP (Table 2) suggested that the Langmuir isotherm gave a good example for the adsorption process. The sorption process would adhere to the Langmuir adsorption equation if the metal ions were taken up separately on a single type of binding site so that the uptake of the first metal ion does not affect the sorption of the following ion.

The sorption capacity, Q_m which is a measure of the maximum adsorption capacity corresponding to complete monolayer coverage showed that the order of adsorption affinity on WHLP was $Zn^{2+} > Pb^{2+} = Co^{2+} > Ni^{2+}$and WHRP was $Pb^{2+} > Co^{2+} > Zn^{2+} > Ni^{2+}$.

Considering that the adsorption of metals in water hyacinth leaves and roots powders is mainly due to ion – exchanges at the surface level, it is expected that more electronegative metal ions will show a higher adsorption tendency [50]. Owing that the electronegativities of metal ions are 2.33, 1.91, 1.65, and 1.88, for Pb^{2+}, Ni^{2+}, Zn^{2+}, and Co^{2+} respectively, therefore, the order of

electronegativity did not match the observed adsorption affinity of metals resulting from Q_m values [51]. Considering the ionic radius of each of the metal ions, approximately given as Pb^{2+}, Ni^{2+}, Zn^{2+}, and Co^{2+} are 119 pm, 83 pm, 74 pm, and 79 pm respectively, therefore, the metals having a larger ionic radius adsorb more effectively than those with a lower ionic radius [52]. However, the adsorption of Zn^{2+} onto PWHL was greater than that of Pb^{2+}, Ni^{2+}, and Co^{2+}; while the greatest adsorption onto PWHR was greatest in Pb^{2+} and Co^{2+}. The high adsorption capacity of Pb^{2+} compared to other metal ions could be due to their lower binding energies [53].

The adsorption coefficient K_a (l/mg) which is related to the apparent energy of sorption was also given in Tables 1-2. The order of favorable energy of adsorption for the water hyacinth leaves was Pb^{2+}> Zn^{2+}> Ni^{2+}> Co^{2+} while for water hyacinth roots it was in the order of Pb^{2+}> Zn^{2+}> Co^{2+}> Ni^{2+}. The result shows that the energy of sorption is more favorable for the sorption of Pb onto the biosorbents than the other metal ions as the K_a values are higher.

The dimensionless constant K_R (Eqn. 3), also known as the separation factor, equilibrium factor, or equilibrium parameter, can be used to explain the fundamental property of the Langmuir isotherm.

$$K_R = \frac{1}{1+ K_a \cdot C_0} \qquad (3)$$

here C_0 is the initial metal ion concentration (mg/L), K_a is the Langmuir constant, and K_R is the dimensionless constant separation factor. The K_R values reveal the isotherm's form. According to the separation factor value, the isotherm's shape can be categorized as follows; $K_R > 1$ indicates unfavorable adsorption, $K_R = 0$ indicates linear adsorption, $0 < K_R < 1$ indicates favorable adsorption, and $K_R < 0$ indicates irreversible adsorption. For this study, the values of K_R obtained for all the metal ions and adsorbents used revealed that the adsorption was favorable as K_R values were greater than 0 but less than 1.

Table 1. The parameters of the Langmuir and Freundlich isotherms for the adsorption of metal ions by WHLP and WHRP

	Langmuir isotherm parameters				**Freundlich isotherm parameters**			
	K_a	Q_m	K_R	R^2	1/n	n	K_f	R^2
Pb^{2+}	10.95	1.06	0.02	0.974	0.607	1.65	2.10	0.990
Ni^{2+}	0.23	0.66	0.47	0.962	0.554	1.81	0.13	0.990
Zn^{2+}	0.42	1.58	0.32	0.981	0.788	1.27	0.45	0.988
Co^{2+}	0.29	1.06	0.41	0.893	0.647	1.55	0.23	0.994

Table 2. The parameters of the Langmuir and Freundlich isotherms for the adsorption of metal ions by WHLP and WHRP

	Langmuir isotherm parameters				**Freundlich isotherm parameters**			
	K_a	Q_m	K_R	R^2	1/n	n	K_f	R^2
Pb^{2+}	2.69	1.43	0.07	0.925	0.72	1.39	1.51	0.994
Ni^{2+}	0.25	0.64	0.44	0.986	0.56	1.80	0.14	0.977
Zn^{2+}	1.08	1.02	0.16	0.987	0.63	1.60	0.50	0.983
Co^{2+}	0.14	1.36	0.59	0.948	0.78	1.29	0.16	0.989

3.6.2. Freundlich isotherm

The Freundlich equation is an empirical equation with no basis in theory, which adopts an exponential variation in site energies and also presumed that surface adsorption is not the rate-limiting step [54]. The rearranged Freundlich adsorption isotherm model for evaluating the non-ideal adsorption involving heterogeneous adsorption phenomena was evaluated by the linearized equation (Eqn. 4) below:

$$log q_e = log K_f + \frac{1}{n} \times log C_e \qquad (4)$$

where 1/n and K_f are empirical constants.

The plots of Freundlich isotherms for the adsorption of Pb^{2+}, Co^{2+}, Zn^{2+}, and Ni^{2+} by WHLP and WHRP are shown in Fig. S3a-d and Fig. S4a-d respectively. The linear plot of the $log q_e$ against $log C_0$ indicates that the adsorption of the sampled metal ions by WHLP and WHRP fits well with the Freundlich model.

The Freundlich isotherm parameters 1/n, n, K_f, and R^2 of all the four metal ions and the adsorbents were captured in Tables 1-2. The R^2 values obtained ranging from 0.983 to 0.994 and 0.977 to 0.994 for WHLP and WHRP respectively for all the metal ions showed that the Freundlich isotherm provided a good model for the sorption process. Considering that n values between 1 and 10 represent beneficial adsorption, all the n values obtained in this study for all the four metal ions on the adsorbents lie between 1 and 10 and are therefore beneficial.

In addition, the effectiveness of the adsorption will shift more over the range of equilibrium concentrations if 1/n is greater. The change in adsorbed concentration is also greater than the change in solute concentration when 1/n > 1.0. Additionally, values of 1/n less than unity show that significant adsorption occurs at low concentrations, but that as the concentrations rise, the amount adsorbed increases less significantly and vice versa. From this study, the value of 1/n obtained for the four metal ions on the adsorbents was found to be less than unity, which agrees with the results discussed above on the decrease in the percentage adsorbed with an increase in concentration.

The adsorption capacity K_f gotten for the various metal ions and adsorbents shows that the array of adsorption for WHLP was Pb^{2+}> Zn^{2+}> Co^{2+} Ni^{2+} while for WHRP it was in the order of Pb^{2+}> Zn^{2+}> Co^{2+}> Ni^{2+}.

In comparing the K_f values for the different adsorbents used, Pb^{2+} WHLP have the highest value of 2.10. For Ni^{2+} the least value (0.14) was observed for WHLP while WHLP had the least value (0.45) for Zn^{2+}. For Co^{2+}, WHRP displayed the least value of 0.16. This confirms that WHLP have a higher adsorption capacity for Pb^{2+} than WHRP.

3.7 Kinetics of biosorption

The kinetic parameter aids in the estimation of the adsorption rate and offers crucial details for process design. The pseudo-first order and pseudo-second order kinetic models are used to assess the data on the kinetics of the adsorption.

3.7.1 Pseudo-first order model

The kinetic rate expression of the first-order model is given as (Eqn. 5):

$$\log(q_e - q_t) = log q_e - \frac{k_1}{2.303} \times t \qquad (5)$$

where q_t and q_e are the amounts of adsorbate (mg/g) at time t (min) and equilibrium respectively. The constant k_1 can be obtained from the slope of the plot of log (q_e – q_t) versus t.

The plots of log(q_e - q_t) versus t for Pb^{2+}, Ni^{2+}, Zn^{2+}, and Co^{2+} for the adsorbents used are shown in Fig. S5a-d and Fig. S6a-d. Tables 3–4 display the pseudo–first order parameters k_1, q_e (calculated), and the regression coefficient (R^2). The first-order model is not suitable to describe the adsorption process, according to the R^2 values obtained. Considering the rate constant k_1, it can be observed that the rate order for water hyacinth leaves was $Pb^{2+} > Ni^{2+} > Co^{2+} > Zn^{2+}$, while for water hyacinth roots, the order was $Ni^{2+} > Co^{2+} > Pb^{2+} > Zn^{2+}$. The value of q_e (calculated) for all the adsorbents differs greatly from those of the experimental. This is to be expected because the adsorption process cannot be described by the pseudo-first order.

Table 3. WHLP pseudo-first order characteristics for the adsorption of metal ions

	Pseudo first order parameters			
Metal ions	q_e (exp.) mg/g	q_e (calc.) mg/g	k_1 (1/min)	R^2
Pb^{2+}	0.1235	0.00014	-0.03	0.063
Ni^{2+}	0.1224	0.00019	-0.04	0.118
Zn^{2+}	0.1249	0.00034	-0.10	0.729
Co^{2+}	0.1244	0.00017	-0.05	0.174

Table 4. WHRP pseudo-first order characteristics for the adsorption of metal ions

	Pseudo first order parameters			
Metal ions	q_e (exp.) mg/g	q_e (calc.) mg/g	k_1 (1/min)	R^2
Pb^{2+}	0.1234	3.76E-05	-0.06	0.248
Ni^{2+}	0.1198	4.76E-03	-0.02	0.016
Zn^{2+}	0.1138	4.34E-05	-0.10	0.486
Co^{2+}	0.1113	1.71E-03	-0.03	0.068

3.7.2. Pseudo-second order

The pseudo-second order model for adsorption kinetics is expressed as (Eqn. 6):

$$\frac{t}{q_t} = \frac{1}{k \cdot q_e^2} + \frac{1}{q_e} t \qquad (6)$$

where k_2 (g/mg·min) is the second-order rate constant.

The second-order rate constants are used to calculate the initial sorption rate, given by (Eqn. 7):

$$h = k_2 \cdot q_e^2 \qquad (7)$$

The plots of t/q_t against t for all the metal ions and all the adsorbents used are shown in Fig. 6a-d and Fig. 7a-d. The projected curves and experimental data points fit together perfectly in the figures. In doing so, they support the idea that chemisorption is the rate-limiting step and that the process follows a pseudo-second order reaction model by providing good linearization of the experimental data [55].

The initial sorption capacity, h, the equilibrium sorption capacity, q_e (calculated), the rate constant, k_2, and the regression coefficient, R^2 were determined from the plot and are shown in Tables S1-S2. The regression coefficient R^2 for the linear plots was higher than 0.995 for all the systems. The equilibrium capacity q_e (calculated) was very close to the experimental q_e. Also, considering the initial sorption rate h, and rate constant, k_2, it can be seen that the order of h and k_2 for WHLP and WHRP was $Pb^{2+} > Co^{2+} > Ni^{2+} > Zn^{2+}$ and $Pb^{2+} > Zn^{2+} > Ni^{2+} > Co^{2+}$ respectively. This implies that Pb^{2+} may be better absorbed by WHLP and WHRP.

All these parameters show good compliance with the pseudo-second order equation. The pseudo-second order rate equation was widely used in the study of adsorption kinetics since reported investigations showed that it was a fairly good fit for the data over the full fractional approach to equilibrium [56, 57].

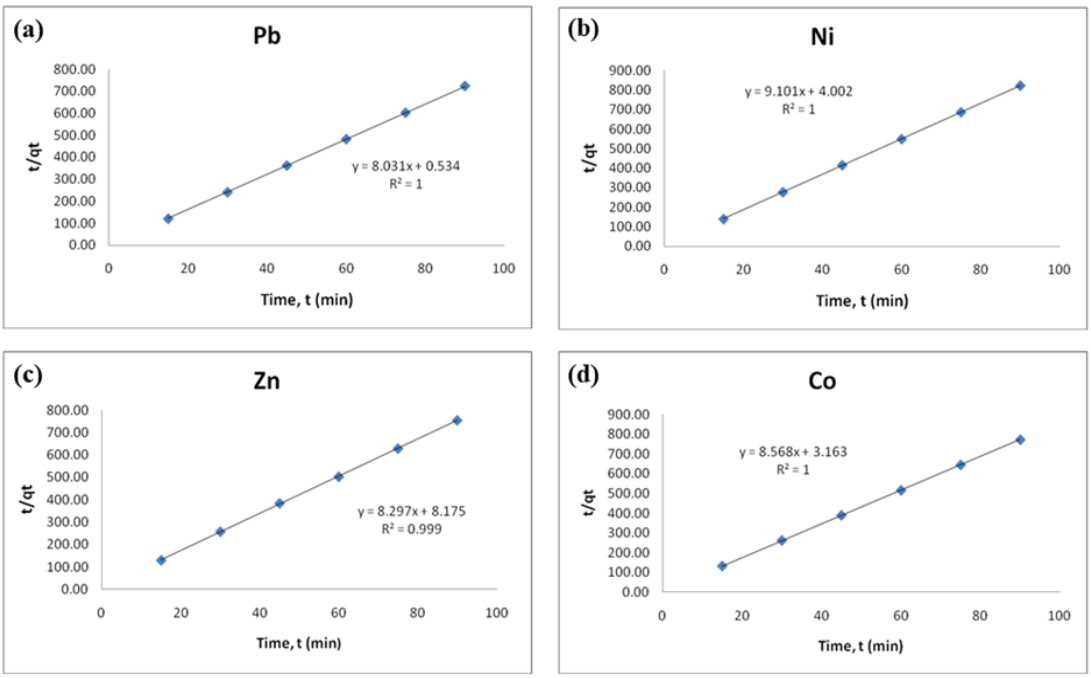

Figure 6. Pseudo-second order for the adsorption of (a) Pb^{2+} (b) Ni^{2+} (c) Zn^{2+} (d) Co^{2+} with WHLP for 5 mg/L of metal and 1 g/25 mL of sorbent

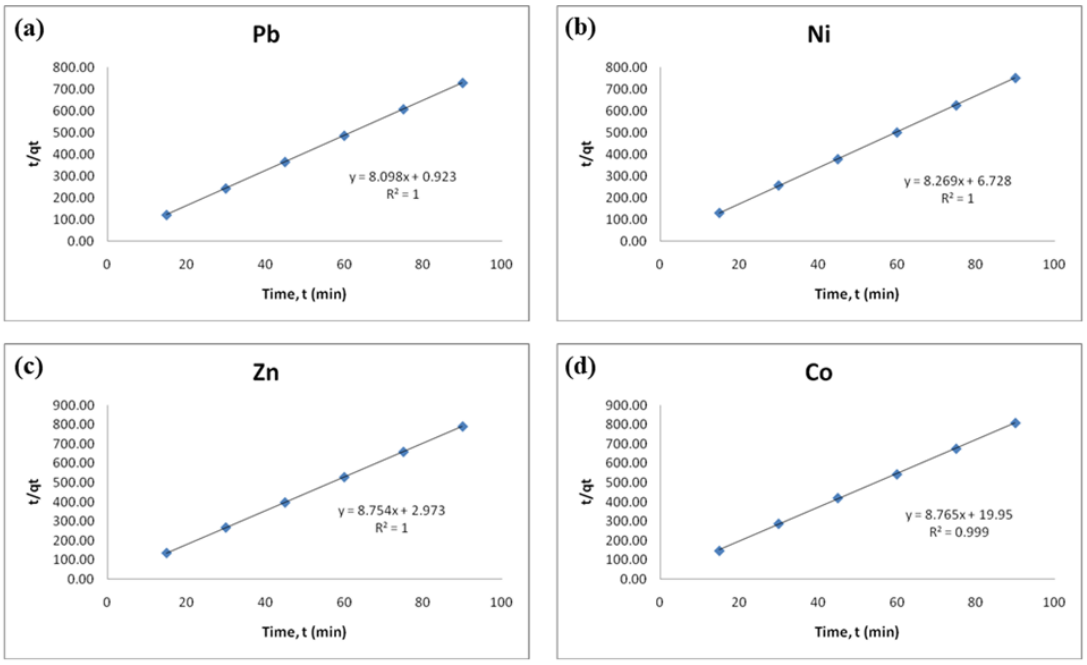

Figure 7. Pseudo-second order for the adsorption of (a) Pb^{2+}, (b) Ni^{2+}, (c) Zn^{2+}, and (d) Co^{2+} with WHRP for 5 mg/L of metal ions and 1 g/25 mL of sorbent

3.8. Desorption studies

After a sorbent material is been used, there is the likelihood of land disposal and incineration. However, these techniques may directly or indirectly harm the environment. However, the recycling of adsorbate and adsorbent may be a strategy for preserving the environment if it were possible to recover metals from the used adsorbent.

For WHLP (**Table S3**), desorption efficiency increases from 9.42 % to 13.04 % for Pb^{2+} as the concentration of NaOH increases from 2 M to 6 M. On the other hand, desorption efficiency increases from 20.43 % to 32.64 % for Ni^{2+}, 52.14 % to 58.49 % for Zn^{2+}, and 16.78 % to 25.46 % for Co^{2+} as the concentration of NaOH increase from 2 M to 4 M. However, when the concentration of NaOH increased from 4 M to 6M desorption efficiency decreased to 28.90 % for Ni^{2+}, 51.94 % for Zn^{2+} and 21.78 % for Co^{2+}. With respect to HNO_3, the desorption efficiency of Pb^{2+} increased from 34.5 % to 35.22 % with an increase in the concentration of HNO_3 from 2 M to 4 M. As the concentration of HNO_3 increased further to 6 M,

desorption efficiency decreased to 33.67 %. Ni^{2+} and Zn^{2+} have a similar trend. There was a decrease in the desorption efficiency of Ni^{2+} and Zn^{2+} from 18.22 % to 16.30 % and 5.25 % to 5.03 % respectively as the concentration of HNO_3 increased from 2 M to 4 M. However, desorption efficiency increased to 17.78 % and 5.65 % for Ni^{2+} and Zn^{2+} respectively with an increase in HNO_3 concentration to 6 M. For Co^{2+}, desorption efficiency increased from 14. 61 % to 15.61 % with an increase in HNO_3 concentration from 2 M to 6 M.

For WHRP (Table S4), desorption efficiency increases with an increase in NaOH concentration for Pb^{2+} and Zn^{2+}. Desorption efficiency increased from 7.2 % to 11.18 % and 4.53 % to 6.38 % for Pb^{2+} and Zn^{2+} respectively as the concentration of NaOH increased from 2 M to 6 M. Desorption efficiency increased from 19.2 % to 29.34 % for Ni^{2+}, and 18.42 % to 27.7 3% for Co^{2+} with an increase in concentration of NaOH from 2 M to 4 M. With the increase in the concentration of NaOH from 4 M to 6 M, desorption efficiency decreased to 28.83 % and 27.33 % for Ni^{2+} and Co^{2+} respectively. With respect to HNO_3, the desorption efficiency of Pb^{2+} increased from 0.68 % to 36.01 % with an increase in HNO_3 concentration from 2 M to 4 M. Increased in concentration from 4 M to 6 M resulted in a decrease in desorption efficiency from 36.01 % to 32.28 %. The desorption efficiency of Ni^{2+} decreased from 20.91 % to 18.89 % with an increase in HNO_3 concentration from 2 M to 4 M. However, with an increase in concentration from 4 M to 6 M, desorption efficiency increased from 18.89 % to 19.23 %. For Zn^{2+} and Co^{2+} desorption efficiency decreases from 9.45 % to 9.35 % and 25.78 % to 24.02 % respectively with an increase in the concentration of HNO_3 from 4 M to 6 M.

Relatively, successful metal ions desorption from the biosorbents was recorded with both NaOH and HNO_3 solutions. The consequential desorption phenomenon seen in both NaOH and HNO_3 may be linked to ion exchange type interaction rather than chemical sorption [34, 58]. These results show that HNO_3 and NaOH can be sufficiently employed in the desorption of the sampled metals from adsorbents.

Desorption does not affect the recycling of used adsorbents. Thus, the use of powdered adsorbents in a suitable combustion chamber (e.g. the boiler at dye works) may be a useful and effective means of disposal. The gaseous products arising from combustion should be trapped using appropriate solvents to avoid air pollution.

4. Conclusions

Herein, we compared the biosorption capacity of WHLP and WHRP in removing metal ions from industrial effluent. Comparatively, the metal ions uptake capacity of WHLP was higher than WHRP as examined by the investigated parameters. This study revealed that Zn^{2+}, Co^{2+}, Pb^{2+} and Ni^{2+} uptake by WHLP and WHRP increased as pH and initial concentration increased and the optimum contact recorded was 60 min. As such, the process follows a pseudo-second order reaction model because it provides good linearization of the experimental data. In addition, biosorption data fitted to both Langmuir and Freundlich isotherms. Overall, this study provides experimental and theoretical insights that could open a new dimension to the exploration of WHLP and WHRP for the efficient removal of metal ions in industrial wastewater.

Conflict of interest

The authors have no conflict of interest to declare.

References

[1]. M. Vhahangwele, L.M. Khathutshelo, Environmental contamination by heavy metals, IntechOpen 32 (2018) 137–144.

[2]. H. Ali, E. Khan, I. Ilahi, Environmental chemistry and ecotoxicology of hazardous heavy metals: Environmental persistence, toxicity, and bioaccumulation, Journal of Chemistry 2019 (2019) 6730305. DOI: 10.1155/2019/6730305

[3]. R.A. Wuana, F.E. Okieimen, Heavy metals in contaminated soils: A review of sources, chemistry, risks and best available strategies for remediation, International Scholarly Research Network Ecology 2011 (2011) 1–20. DOI: 10.5402/2011/402647

[4]. J. Briffa, E. Sinagra, R. Blundell, Heavy metal pollution in the environment and their toxicological effects on humans, Heliyon 6 (2020) e04691. DOI: 10.1016/j.heliyon.2020.e04691

[5]. M. Jaishankar, T. Tseten, N. Anbalagan, B.B. Mathew, K.N. Beeregowda, Toxicity, mechanism and health effects of some heavy metals, Interdisciplinary Toxicology 7 (2014) 60–72. DOI: 10.2478/intox-2014-0009

[6]. S. Mitra, A.J. Chakraborty, A.M. Tareq, T. Bin Emran, F. Nainu, A. Khusro, A.M. Idris, M.U. Khandaker, H. Osman, F.A. Alhumaydhi, J. Simal-Gandara, Impact of heavy metals on the environment and human health: Novel therapeutic insights to counter the toxicity, Journal of King Saud University - Science 34 (2022) 101865. DOI: 10.1016/j.jksus.2022.101865

[7]. Q. Zhou, N. Yang, Y. Li, B. Ren, X. Ding, H. Bian, X. Yao, Total concentrations and sources of heavy metal pollution in global river and lake water bodies from 1972 to 2017, Global Ecology and Conservation 22 (2020) e00925. DOI: 10.1016/j.gecco.2020.e00925

[8]. N. Akhtar, M.I. Syakir Ishak, S.A. Bhawani, K. Umar, Various natural and anthropogenic factors responsible for water quality degradation: A review, Water 13 (2021) 2660. DOI: 10.3390/w13192660

[9]. I.V. Muralikrishna, V. Manickam, Industrial wastewater treatment technologies, recycling, and reuse. Environmental Management 13 (2017) 295-336. DOI: 10.1016/b978-0-12-811989-1.00013-0

[10]. N. Munir, M. Jahangeer, A. Bouyahya, N. El Omari, R. Ghchime, A. Balahbib, S. Aboulaghras, Z. Mahmood, M. Akram, S.M.A. Shah, I.N. Mikolaychik, M. Derkho, M. Rebezov, B.

Venkidasamy, M. Thiruvengadam, M.A. Shariati, Heavy metal contamination of natural foods is a serious health issue: A review, Sustainability. 14 (2022) 161. DOI: 10.3390/su14010161

[11]. Yi Yuan, B.Liu, H. Liu, Spatial distribution and source identifcation for heavy metals in surface sediments of East Dongting Lake, China, Scientific Reports 12 (2022) 7940. DOI: 10.1038/s41598-022-12148-x

[12]. I.B. Obinnaa, E.C. Ebere, A Review: Water pollution by heavy metal and organic pollutants: Brief review of sources, effects and progress on remediation with aquatic plants, Analytical Methods Environmental Chemistry Journal 2 (2019) 5–38. DOI: 10.24200/amecj.v2.i03.66

[13]. L.A.H. Vásquez, F.P. García, J.P. Méndez, A.A. Lass-man, E.M.O. Sánchez, Artificial wetlands and floating islands: Use of macrophytes, South Florida Journal of Development 3 (2022) 476–498. DOI: 10.46932/sfjdv3n1-036

[14]. J. Li, H. Yu, Y. Luan, Meta-analysis of the copper, zinc, and cadmium absorption capacities of aquatic plants in heavy metal-polluted water, International Journal of Environmental Research and Public Health. 12 (2015) 14958–14973. DOI: 10.3390/ijerph121214959

[15]. S. Khan, I. Ahmad, M.T. Shah, S. Rehman, A. Khaliq, Use of constructed wetland for the removal of heavy metals from industrial wastewater, Journal of Environmental Management 90 (2009) 3451–3457. DOI: 10.1016/j.jenvman.2009.05.026

[16]. A. Guittonny-Philippe, V. Masotti, P. Höhener, J.L. Boudenne, J. Viglione, I. Laffont-Schwob, Constructed wetlands to reduce metal pollution from industrial catchments in aquatic Mediterranean ecosystems: A review to overcome obstacles and suggest potential solutions, Environment International 64 (2014) 1–16. DOI: 10.1016/j.envint.2013.11.016

[17]. E. Sanmuga Priya, P. Senthamil Selvan, Water hyacinth (Eichhornia crassipes) – An efficient and economic adsorbent for textile effluent treatment – A review, Arabian Journal of Chemistry 10 (2017) S3548–S3558. DOI: 10.1016/j.arabjc.2014.03.002

[18]. C. Mahamadi, Water hyacinth as a biosorbent: A review, African Journal of Environmental Science and Technology 5 (2012) 1137–1145. DOI: 10.5897/ajestx11.007

[19]. J.A. Coetzee, R.W. Jones, M.P. Hill, Water hyacinth, Eichhornia crassipes (Pontederiaceae), reduces benthic macroinvertebrate diversity in a protected subtropical lake in South Africa, Biodiversity Conservation 23 (2014) 1319–1330. DOI: 10.1007/s10531-014-0667-9

[20]. M. Shah, H.N. Hashmi, A. Ali, A.R. Ghumman, Performance assessment of aquatic macrophytes for treatment of municipal wastewater, Journal of Environmental Health, Science and Engineering 12 (2014) 1–12. DOI: 10.1186/2052-336X-12-106

[21]. J.L. Jones, R.O. Jenkins, P.I. Haris, Extending the geographic reach of the water hyacinth plant in removal of heavy metals from a temperate Northern Hemisphere river, Scientific Reports 8 (2018) 11071. DOI: 10.1038/s41598-018-29387-6

[22]. M. Bilal, T. Rasheed, J.E. Sosa-Hernández, A. Raza, F. Nabeel, H.M.N. Iqbal, Biosorption: An interplay between marine algae and potentially toxic elements - A review, Marine Drugs 16 (2018) 65. DOI: 10.3390/md16020065

[23]. J. Adusei-Gyamfi, B. Ouddane, L. Rietveld, J.P. Cornard, J. Criquet, Natural organic matter-cations complexation and its impact on water treatment: A critical review, Water Research 160 (2019) 130–147. DOI: 10.1016/j.watres.2019.05.064

[24]. A. Yan, Y. Wang, S.N. Tan, M.L. Mohd Yusof, S. Ghosh, Z. Chen, Phytoremediation: A promising approach for revegetation of heavy metal-polluted land, Frontiers in Plant Science 11 (2020) 1–15. DOI: 10.3389/fpls.2020.00359

[25]. A. Saravanan, P.S. Kumar, R. V. Hemavathy, S. Jeevanantham, P. Harikumar, G. Priyanka, D.R.A. Devakirubai, A comprehensive review on sources, analysis and toxicity of environmental pollutants and its removal methods from water environment, Science of the Total Environment 812 (2022) 152456. DOI: 10.1016/j.scitotenv.2021.152456

[26]. T. Mahmood, S.A. Malik, S.T. Hussain, Biosorption and recovery of heavy metals from aqueous solutions by Eichhornia crassipes (water hyacinth) ash, Bioresources 5 (2010) 1244–1256.

[27]. B.B. Mathew, M. Jaishankar, V.G. Biju, Krishnamurthy Nideghatta Beeregowda, Role of bioadsorbents in reducing toxic metals, Journal of Toxicology 2016 (2016). DOI: 10.1155/2016/4369604

[28]. Z. Al-Qodah, M.A. Yahya, M. Al-Shannag, On the performance of bioadsorption processes for heavy metal ions removal by low-cost agricultural and natural by-products bioadsorbent: A review, Desalination and Water Treatment 85 (2017) 339–357. DOI: 10.5004/dwt.2017.21256

[29]. S. De Gisi, G. Lofrano, M. Grassi, M. Notarnicola, Characteristics and adsorption capacities of low-cost sorbents for wastewater treatment: A review, Sustainable Materials and Technologies 9 (2016) 10–40. DOI: 10.1016/j.susmat.2016.06.002

[30]. A.T. Huynh, Y.C. Chen, B.N.T. Tran, A small-scale study on removal of heavy metals from contaminated water using water hyacinth, Processes 9 (2021) 1–9. DOI: 10.3390/pr9101802

[31]. H.A. Hassoon, A.M. Najem, Removal of some traces heavy metals from aqueous solutions by water hyacinth leaves powder, Iraqi Journal of Science 58 (2017) 611–618.

[32]. D. Hemalatha, R.M. Narayanan, S. Sanchitha, Removal of zinc and chromium from industrial wastewater using water hyacinth (E. crassipes) petiole, leaves and root powder: Equilibrium study, Materials Today Proceeding 43 (2020) 1834–1838. DOI: 10.1016/j.matpr.2020.10.725.

[33]. G.O. Tesi, O. Ejeromedoghene, B. Kpomah, A.R. Ipeaiyeda, Sorption of Mn(II) ions from wastewater using dried and blended water hyacinth (*Eichhornia crassipes*) roots: Adsorption-desorption studies and kinetics, Journal of the

Turkish Chemical Society Section A: Chemistry 11 (2024) 415-424.
[34]. A.R. Ipeaiyeda, G.O. Tesi, Sorption and desorption studies on toxic metals from brewery effluent using eggshell as adsorbent, Advances in Natural Science 7 (2014) 15–24. DOI: 10.3968/5394
[35]. H.D. Utomo, K.X.D. Tan, Z.Y.D. Choong, J.J. Yu, J.J. Ong, Z.B. Lim, Biosorption of heavy metal by algae biomass in surface water, Journal of Environmental Protection 07 (2016) 1547–1560. DOI: 10.4236/jep.2016.711128
[36]. H. Shokry, M. Elkady, E. Salama, Eco-friendly magnetic activated carbon nano-hybrid for facile oil spills separation, Scientific Reports 10 (2020) 1–18. DOI: 10.1038/s41598-020-67231-y
[37]. J.M. Zhou, Z.C. Jiang, X.Q. Qin, L.K. Zhang, Q.B. Huang, G.L. Xu, Effects and mechanisms of calcium ion addition on lead removal from water by *Eichhornia crassipes*, International Journal of Environmental Research and Public Health 17 (2020) 928. DOI: 10.3390/ijerph17030928
[38]. J. Weißpflog, A. Gündel, D. Vehlow, C. Steinbach, M. Müller, R. Boldt, S. Schwarz, D. Schwarz, Solubility and selectivity effects of the anion on the adsorption of different heavy metal ions onto chitosan, Molecules 25 (2020) 2482. DOI: 10.3390/molecules25112482
[39]. A.M. Najem, Evaluation the biosorption capacity of water hyacinth (Eichhornia crassipes) root for some heavy metals, Iraqi Journal of Science 56 (2015) 2846–2852.
[40]. B.S. Smolyakov, Uptake of Zn, Cu, Pb, and Cd by water hyacinth in the initial stage of water system remediation, Applied Geochemistry 27 (2012) 1214–1219. DOI: 10.1016/j.apgeochem.2012.02.027
[41]. D.M. Hammad, Cu, Ni and Zn phytoremediation and translocation by water hyacinth plant at different aquatic environments, Australia Journal of Basic and Applied Sciences 5 (2011) 11–22.
[42]. H. Singh, S. Choden, Comparison of adsorption behaviour and kinetic modeling of bio-waste materials using basic dye as adsorbate, Indian Journal of Chemical Technology 21 (2014) 359–398.
[43]. I. Michalak, K. Chojnacka, A. Witek-Krowiak, State of the art for the biosorption process - A review, Applied Biochemistry and Biotechnology 170 (2013) 1389–1416. DOI: 10.1007/s12010-013-0269-0
[44]. E. Torres, Biosorption: A review of the latest advances, Processes 8 (2020) 1–23. DOI: 10.3390/pr8121584
[45]. W. Jiang, Y. Hu, Z. Zhu, Biosorption characteristic and cytoprotective effect of Pb^{2+}, Cu^{2+} and Cd^{2+} by a novel polysaccharide from Zingiber strioatum, Molecules. 27 (2022) 8036. DOI: 10.3390/molecules27228036
[46]. F. Gorzin, M.M. Bahri Rasht Abadi, Adsorption of Cr(VI) from aqueous solution by adsorbent prepared from paper mill sludge: Kinetics and thermodynamics studies, Adsorption Science and Technology. 36 (2018) 149–169. DOI: 10.1177/0263617416686976
[47]. P.E. Ohale, C.E. Onu, N.J. Ohale, S.N. Oba, Adsorptive kinetics, isotherm and thermodynamic analysis of fishpond effluent coagulation using chitin derived coagulant from waste Brachyura shell, Chemical Engineering Journal Advances 4 (2020) 100036. DOI: 10.1016/j.ceja.2020.100036
[48]. T.G. Ambaye, M. Vaccari, E.D. van Hullebusch, A. Amrane, S. Rtimi, Mechanisms and adsorption capacities of biochar for the removal of organic and inorganic pollutants from industrial wastewater, International Journal of Environmental Sciences and Technology 18 (2021) 3273–3294. DOI: 10.1007/s13762-020-03060-w
[49]. M. Matouq, N. Jildeh, M. Qtaishat, M. Hindiyeh, M.Q. Al Syouf, The adsorption kinetics and modeling for heavy metals removal from wastewater by Moringa pods, Journal of Environmental Chemical Engineering 3 (2015) 775–784. DOI: 10.1016/j.jece.2015.03.027
[50]. J.C. Zheng, H.Q. Liu, H.M. Feng, W.W. Li, M.H.W. Lam, P.K.S. Lam, H.Q. Yu, Competitive sorption of heavy metals by water hyacinth roots, Environmental Pollution 219 (2016) 837–845. DOI: 10.1016/j.envpol.2016.08.001
[51]. D. Kołodyńska, J. Krukowska, P. Thomas, Comparison of sorption and desorption studies of heavy metal ions from biochar and commercial active carbon, Chemical Engineering Journal 307 (2017) 353–363. DOI: 10.1016/j.cej.2016.08.088
[52]. G.M. Al-Senani, F.F. Al-Fawzan, Adsorption study of heavy metal ions from aqueous solution by nanoparticle of wild herbs, Egyptian Journal of Aquatic Research. 44 (2018) 187–194. DOI: 10.1016/j.ejar.2018.07.006
[53]. M. Zhao, Y. Dai, M. Zhang, C. Feng, B. Qin, W. Zhang, N. Zhao, Y. Li, Z. Ni, Z. Xu, D.C.W. Tsang, R. Qiu, Mechanisms of Pb and/or Zn adsorption by different biochars: Biochar characteristics, stability, and binding energies, Science of the Total Environment 717 (2020) 136894. DOI: 10.1016/j.scitotenv.2020.136894
[54]. K.S. Padmavathy, G. Madhu, P.V. Haseena, A study on effects of pH, adsorbent dosage, time, initial concentration and adsorption isotherm study for the removal of hexavalent chromium (Cr (VI)) from wastewater by magnetite nanoparticles, Procedia Technology 24 (2016) 585–594. DOI: 10.1016/j.protcy.2016.05.127
[55]. Q. Wang, Y. Wang, Z. Yang, W. Han, L. Yuan, L. Zhang, X. Huang, Efficient removal of Pb(II) and Cd(II) from aqueous solutions by mango seed biosorbent, Chemical Engineering Journal Advances 11 (2022) 100295. DOI: 10.1016/j.ceja.2022.100295
[56]. H. Tounsadi, A. Khalidi, M. Abdennouri, N. Barka, Biosorption potential of Diplotaxis harra and Glebionis coronaria L. biomasses for the removal of Cd(II) and Co(II) from aqueous solutions, Journal of Environmental and Chemical

Engineering 3 (2015) 822–830. DOI: 10.1016/j.jece.2015.03.022
[57]. E.D. Revellame, D.L. Fortela, W. Sharp, R. Hernandez, M.E. Zappi, Adsorption kinetic modeling using pseudo-first order and pseudo-second order rate laws: A review, Cleaner Engineering and Technology 1 (2020) 100032. DOI: 10.1016/j.clet.2020.100032
[58]. D.L. Gómez-Aguilar, J.A. Esteban-Muñoz, J.P. Rodríguez-Miranda, D. Baracaldo-Guzmán, O.J. Salcedo-Parra, Desorption of coffee pulp used as an adsorbent material for Cr(III and VI) ions in synthetic wastewater: A preliminary study, Molecules 27 (2022) 2170. DOI: 10.3390/molecules27072170.

Received: 15.07.2024
Received in revised form: 05.02.2025
Accepted: 06.02.2025